

Proprietary of Total Intensity Magnetic Data to Detect the Subsurface Structures and Tectonics of Southern Sinai Peninsula, Egypt

Ahmed A. El-Khafeef¹ and Shadia T. El Khodary^{2*}

¹Exploration Dept., Egyptian Petroleum Research Institute, Nasr City, Cairo, Egypt.

²Geology Dept., Faculty of Science, Tanta University, Tanta, Egypt.

*s_elkhodary@hotmail.com

Abstract: This study presents the analysis and interpretation of magnetic data to map the subsurface structural framework of the present area. Structural interpretation of the magnetic data was achieved through applying advanced processing techniques that provide automatic delineation and depth estimation of the magnetic structures. Some structural elements could be deduced from the qualitative interpretation of such magnetic anomalies. Phase-shifts of magnetic anomalies due to the local direction of the geomagnetic field vector can be corrected using a reduction-to-pole filtering operation. At the interpretation stage, the analysis of the RTP magnetic data, which included low-pass/high-pass filtering by power spectrum and separation of the magnetic causatives of shallow sources from those of deeper sources through the matching band-pass filtering. The horizontal gradient and local wave number tools were used for locating the magnetic sources and their properties. In this case, peaks in those methods can be used to locate sources representing the edges of thin horizontal sheets and estimate their strike directions which, used to delineate the tectonic framework of the investigated area. The shallow structural depths located between 1.5 to 2.5 km (red color) dominate the majority of the southern part, as well as some parts in the northern part. While the deep depths 2.5 to 5.5 km (blue color) dominate the northcentral and westcentral parts. The mapped structures reveal that, the area is affected by a set of faults trending mainly in the NE-SW, NW-SE and N-S directions. Moreover, the area is dissected by a set of deep basement swells and troughs, as well as shallow anticlinal and synclinal trends controlled mainly by the predominant faults.

[Ahmed A. El-Khafeef and Shadia T. El Khodary. **Proprietary of Total Intensity Magnetic Data to Detect the Subsurface Structures and Tectonics of Southern Sinai Peninsula, Egypt.** Journal of American Science 2011;7(3):453-463]. (ISSN: 1545-1003). <http://www.americanscience.org>.

Keywords: Proprietary; Magnetic Data; Subsurface Structure; Tectonics; Southern Sinai Peninsula; Egypt

Introduction:

The study area occupies nearly the southern half of Sinai Peninsula, that located between the Gulf of Suez and Gulf of Aqaba. It lies between latitudes 27° 50' & 29° 30' N and longitudes 33° 00' & 34° 45' E (Fig.1) . It is noticed that, the concerned area is an active seismic area, the higher rate of seismic activities at the southern end of the Gulf of Suez is interpreted as a result of the triple junction between the African and Arabian plates and Sinai subplate (Ben-Menahem, 1979). This region is considered as a Tertiary cratonic rift between Northeastern Africa and the Arabian Peninsula, its rifting phase ceased when continental separation became more oblique, due to the predominant movements of the left-lateral transform fault, that extends north north-eastward through the Gulf of Aqaba to the Dead Sea (Patton et al., 1994, USGS 1998 and Reilinger et al., 2006).

Many geophysical researches have been applied on this area to delineate the subsurface structures and tectonism. It was indicated that, the structures of the study area are related to the Gulf of Suez and the Red Sea tectonics. These structures extend from the basement rocks upwards into the

sedimentary sequences and divided the area into several major faulted blocks, that have great importance in sealing the oil traps (Rabeh, 2003). It was noticed that, the southern part of Sinai Peninsula tends to move towards the east (NNE) at an angle smaller than that of the northern part (Rabeh et al., 2008).

In general, the geophysical magnetic method is mainly based on the measurements and analysis of small variations in the earth's magnetic field within any area. An aeromagnetic map is a reflection of the distinctions in the magnetic properties of the underlying rocks. So, these variations encountered in the measured magnetic field are attributed to the distribution of the subsurface magnetically-polarized rocks. The sedimentary rocks are of weaker magnetic properties than the underlying basement rocks, especially the mafic rocks. Therefore, the magnetic methods are used to delineate the structural and lithological configuration of the basement rocks.

The main available type of geophysical data for the current study is a magnetic map reflecting the distribution of the total intensity magnetic anomalies within the study area (Fig. 4). The current study deals

with the interpretation of land- magnetic data of South Sinai to map the subsurface structures and the tectonic setting of the area.

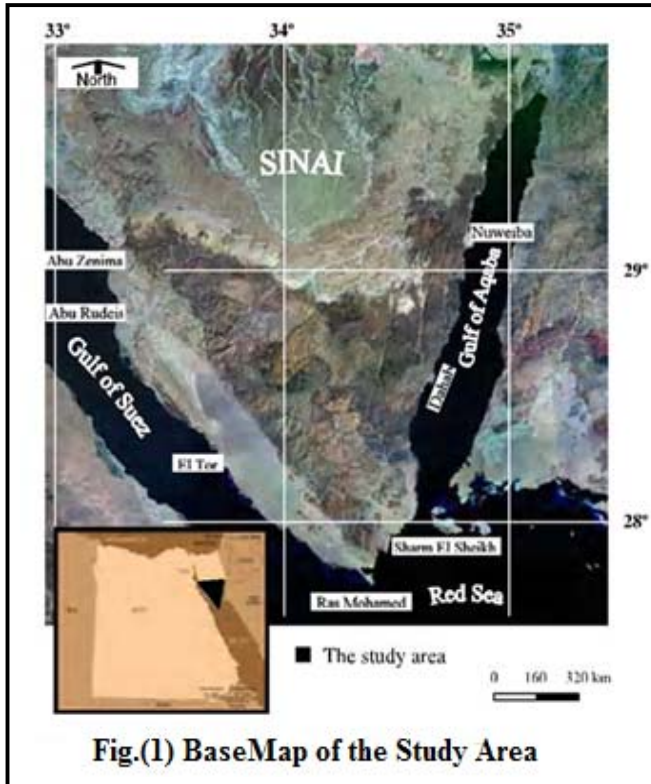


Fig.(1) BaseMap of the Study Area

Geological Outlines

Sinai Peninsula displays a variety of simple and complex structural forms, so it is considered the glamorous region from the geological stand point of view (Abu-Al-Izz,1971).

Geomorphologically, South Sinai is characterized by elevated mountains district assuming a triangular shape with its apex at Ras Mohamed to the south, and a central plateau in the form of two main questas, El Egma to the southwest, and El Tieh to the north (Abu –Al-Izz,1971).

The surface rock units of the study area range from Pre-Cambrian basement rocks to the Quaternary deposits (Fig.2). The basement rocks (Precambrian) are located in the southern region of the area, while the Paleozoic rocks are located in the middle area and the Mesozoic rocks occupy the eastern and western parts of the study area. The Quaternary deposits lie on either sides of the Precambrian rocks along the Gulf of Suez and Gulf of Aqaba. The basement rocks of South Sinai are gently dipping northward, with a consequent thickening of the overlying sediments.

Structurally, both the basement rocks and the thin sedimentary cover exhibit a large number of

surface tectonic elements of varying lengths and trends (Fig., 3), as shown by Neev, 1975, Agha,1981 and Said,1990. Ahmed and Hassaneen (1985) had addressed the predominant directions of the fault systems in Sinai, through the interpretation of the magnetic map of Egypt. They summarized the directions into the following categories:

- 1) The N-S direction is predominant.
- 2) The E-W direction (Mediterranean Sea trend).
- 3) The NE-SW direction is presented by five directions, which are 10°, 25°,45°,50°and 70°from the north (ENE is the Syrian Arc trend and NNE is the Gulf of Aqaba trend).
- 4)The NW-SE direction is represented by three directions, which are 15°,25° and 40° from the north (Gulf of Suez trend).

Tectonically, the wrenching along the Gulf of Aqaba is reflected in the form of strike-slip faults cutting through the basement rocks and the overlying sedimentary section, as well as en-echelon folds (Abdel Khalek et al., 1993). The northward extension of the Gulf of Aqaba leads to the Dead Sea –Jordan transform fault system, which links the Arabian Plate convergence in Southern Turkey with the active seafloor spreading in the Red Sea. The Aqaba – Levant structure is thought to have formed by left-lateral shear motion (Freund et al.,1970) with relative displacement ranges from tens of meters up to 9.8 km. The creation of the pull-apart basins is mainly related to strike-slip motion (Garfunkel,1981) with N-S to NNE-SSW fault trend (Lyberis,1988).

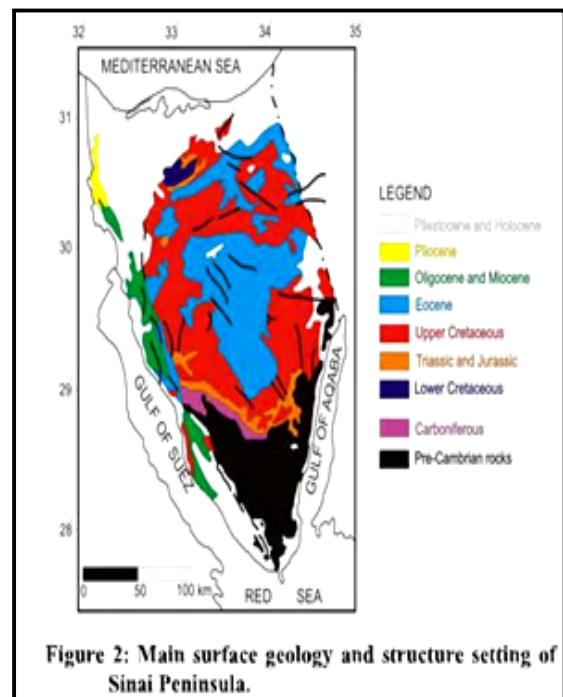


Figure 2: Main surface geology and structure setting of Sinai Peninsula.

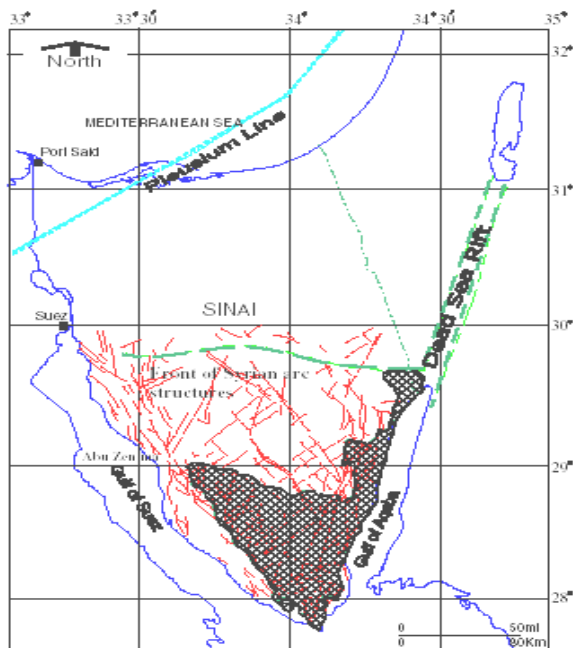


Fig.(3) Tectonic map of South Sinai (modified after Neev 1975 and Agha 1981)

Main Concepts

There are some principles should be taken into consideration when working with the magnetic data. The interpretation of magnetic data is not unique, because it is controlled by many factors; for example, depth to top of the causative feature, its shape, its azimuth, its magnetic susceptibility, that is mainly related to its petrographical composition. Such factors are related to the subsurface anomalous features, that produce their magnetic signatures at the surface. The availability and use of some of these factors during the interpretation reduce the ambiguity in the magnetic interpretation. Such factors can be taken from the available well data and regional geology of the area. The available magnetic data for this study have been corrected for the diurnal variations, instrument drift, and for the errors in positioning and height keeping.

Insights On The Original Magnetic Data

The close study of the total intensity map with scale of 1:500000 and 30 nT contour interval (Ismail et al. 2001) (Fig. 4) indicates that, most of the observed anomalies show NE-SW, NW-SE and N-S trend patterns with some sharp gradients at varying locations. Since the magnetic maps are related directly to the basement rock features, so this indicates the presence of a basement relief change.

Close investigation of the total intensity land magnetic map (Fig. 4) revealed that, the western side of the map is occupied by three positive elongated

anomalies intervened by two negative ones, all are trending NW-SE. The northern part of the area seems to be affected by three high positive large extent anomalies, which are oval shaped trending E-W. The southern area of the map is characterized by a large E-W high amplitude anomaly, along with a small round NE-SW positive anomaly. The central and eastern parts of the area are characterized by the presence of large number of negative anomalies trending E-W, ENE-WSW and N-S directions. These negative anomalies may be due to lithologic variation of the basement rocks and or due to the faulting process in this part. There is a large oval shape positive anomaly occupies the central part of the mapped area trending NNE-SSW direction, which may be referred to shallow structure or high magnetic susceptibility feature.

Magnetic Data Processing

The processing of the magnetic anomalies is based on the analysis of the computer-digitized information using different processing techniques at different altitudinal levels from the compiled total magnetic data shown in Figure (4). These techniques involve; first the reduction to the north magnetic pole. The reduced to the north magnetic pole digitized data were used for additional investigative techniques, that helped integrative to deduce the structural set-up for the basement of considered area.

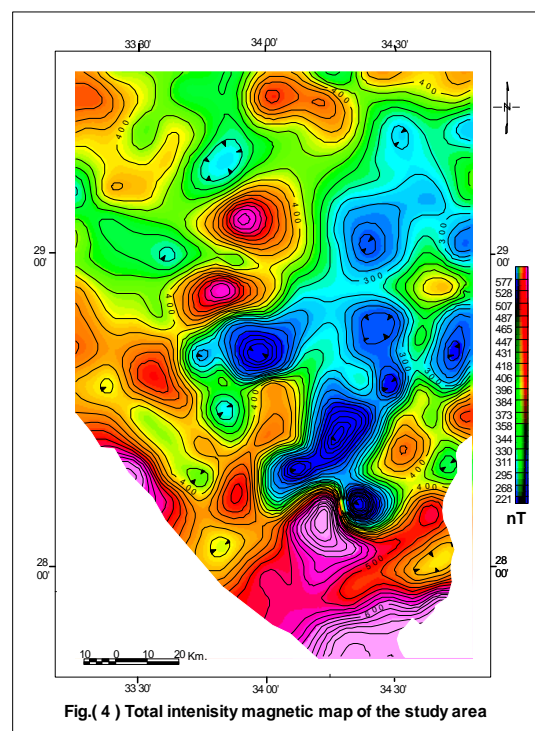


Fig.(4) Total intensity magnetic map of the study area

The Reduction to the North Magnetic Pole:

A reduction-to-pole (RTP) transformation is typically applied to the total magnetic data to minimize the polarity effects (Blakely, 1995). Reduction-to-the-pole is a filtering technique used to align the peaks and gradients of magnetic anomalies directly over their sources. These effects are manifested as a shift of the main anomaly from the center of the magnetic source and are due to the vector inclination and declination of the measured magnetic field. The RTP alteration usually involves an assumption that, the total magnetizations of most rocks align parallel or anti-parallel to the Earth's main field (declination= 2.38° , inclination= 42.32° and IGRF total intensity value= 42803 nT, for the study area). In the present study, the total intensity land magnetic anomaly data are reduced to the magnetic pole (RTP), according to Geosoft Oasis Montaj (2007).

Inspection of the RTP map (Fig.5) shows that, the southern and southeastern parts of the area are characterized by the presence of a very high amplitude oval shape positive anomaly trending NNW-SSE, together with an elongated one having a big aerial extent trending E-W. This region represents the basement rocks lying between the two gulfs, expressing their structural directions. While the western area of the map shows a high positive amplitude anomaly, comprising three small oval shape ones trending NW-SE direction parallel to the Gulf of Suez with moderately steep gradient, indicating intermediate depth sources. The central and northeastern parts of the area are characterized by very low amplitude anomalies trending NNE-SSW and N-S directions, with almost oval shape.

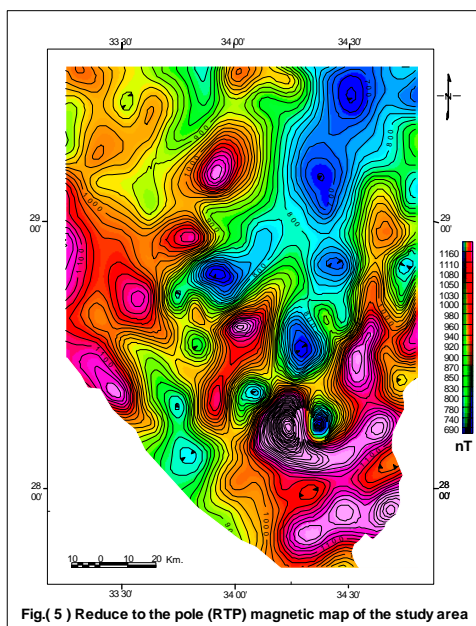


Fig.(5) Reduce to the pole (RTP) magnetic map of the study area

1-Low-pass and High-pass filtering of the RTP Magnetic Data

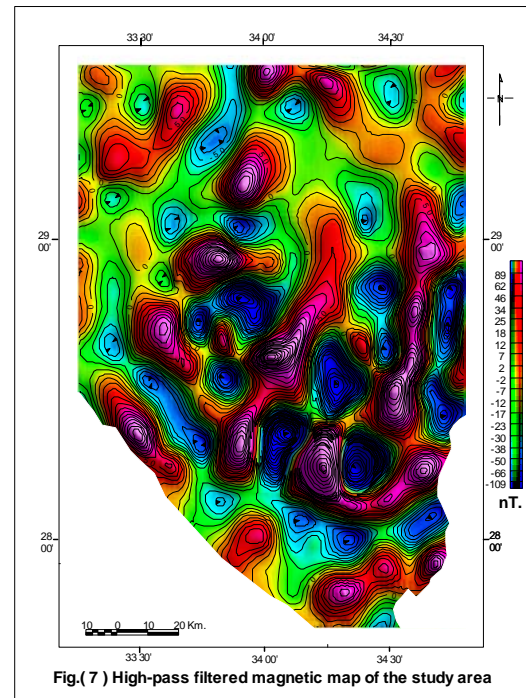
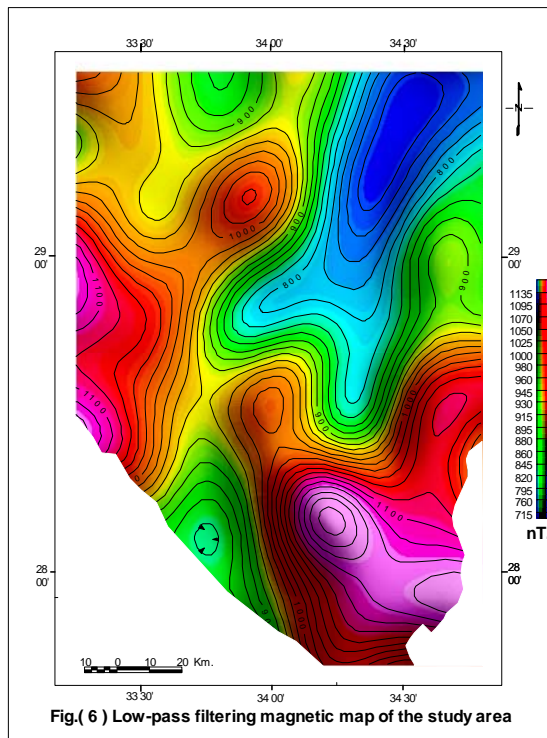
Filtering the magnetic data is an essential process prior to the analysis and interpretation. The objective of the filter is to recondition the data set and to render the resulting presentation in such a way as to make it easier to interpret the significance of anomalies in terms of their geological sources. Therefore, the most effective way to filter the data is through understanding the geologic control and the desired filtered results. Several filtering techniques can be performed in the frequency domain. However, one of the most traditional filters, used in the potential field, is the separation of long (deep) and short (shallow) wavelength anomalies. The success of this technique depends on the proper choice of the cut-off wavelength used in the filter design. The cut-off wavelengths and information about the contribution of the short and long wavelengths in the spectrum can be obtained from the calculated radially-averaged power spectrum of the data.

Two-dimensional power spectrum curve of the present RTP data, using Geosoft Oasis Montaj (2007), shows two linear segments related to the long and short wavelength components with frequency bands ranges from 0.0 to 0.3 and from 0.3 to 0.95 wavenumber, respectively. Following Spector and Grant (1970), the slope, of these two linear segments were used to estimate the average depths to the tops of the deep-seated and near-surface magnetic sources, respectively. These depths are average estimates for the entire area and do not reflect a resolved and detailed such topography of the basement surface. The frequency bands corresponding to these linear segments were used through the band pass filter technique to produce the low-pass and high-pass magnetic component, maps (Figs.6 & 7).

The regional (low-pass) magnetic anomaly map (Fig.6) is characterized by large, homogenous and high amplitude anomalies, which are caused by deep-seated causatives. Inspection of this map indicates that, broad and oval shape high intensity negative magnetic anomalies extend from the northeastern corner to the central part of the area. This belt trends in the NE-SW direction and degrades by steep gradients. The southeastern corner of the mapped area is characterized by a broad aerial extent and high intensity positive magnetic anomaly with elongated shape, trending in the NW-SE direction. It is surrounded by steep magnetic gradients from its northern and western sides, indicating the existence of major deep-seated faults around this anomaly from both sides. Broad positive magnetic anomalies with oval shape occupy the western part of the study area with gentle magnetic gradients trending NNE-SSW.

Residual (high-pass) magnetic anomalies map (Fig.7) are of primary importance in reflecting the structures presented on the basement surface or the magnetic sources occurred within the sedimentary cover. Examination of such map revealed that, the map is characterized by high frequencies, short wavelengths, small size, weak intensity, sharp low amplitude and nearly round-shaped anomalies. The

southern part of the study area is characterized by numerous positive and negative small elongated to round shaped, and high amplitude anomalies, trending in the NE-SW, N-S and E-W directions. The central and northern parts have large elongated and nearly rounded anomalies, trending in the NE-SW and N-S directions.



2-Extracting the magnetic sources using matched bandpass filtering

The idea of matched filtering is to fit the Fourier power spectrum of the workable aeromagnetic data with a series of equivalent power spectra corresponding to simple magnetic layers in the earth (Syberg, 1972).

Typically, there will be a noise layer containing low-amplitude, very short-wavelength magnetic noises largely unrelated to geologic sources, a layer corresponding to the near-surface magnetic sources and one or more layers corresponding to the deeper magnetic sources.

The matched bandpass filtering (Phillips, 2000) is a technique used to separate the magnetic anomalies produced at different source depths. In particular, anomalies produced by near-surface sources, such as shallow geologic units and cultural features can be separated from anomalies produced by deeper geologic units. Normally, the aeromagnetic signals produced from the near-surface sedimentary

geologic units and cultural (man-made) features will have much lower amplitudes and much shorter wavelengths than the aeromagnetic signals resulted from the deeply buried crystalline geologic units within the basement rock. In this situation, the Fourier band-pass filtering can be used to isolate and enhance the anomaly wavelengths associated with the shallow (or deep) sources. This is reflected by varying slopes in the Fourier power spectrum of the aeromagnetic data, which has been averaged for all azimuths.

The RTP magnetic map of the study area (Fig.5) can be used to illustrate this process (using MFDESIGN and MFFILTER programs of Phillips, 1997). Figure (8) contains the RTP anomalies produced by shallow geological sources with equivalent dipole layer for this band pass located at 0.487km. The intermediate wavelength map (Fig.9) involves the RTP anomalies resulted by geologic sources at depth nearly of 1.5 km. Moreover, the long wavelength RTP map (Fig.10) includes the anomalies

inferred from the deepest and broadest features of the section at depth of about 5.4 km.

Automated Interpretation of Source Parameters

Various methods are elaborated for estimating the source locations and other source parameters from total magnetic data, both in profile form and in map form. This section compares the results of two analogous interpretation methods, that work on map data: the horizontal gradient method and the local wavenumber method.

1- Horizontal Gradient Magnitude (HGM)

Horizontal gradient is a simple approach to locate linear structures, such as contacts and faults from potential field data. For magnetic field $M(x,y)$, the horizontal gradient magnitude $HG(x,y)$ is given by Cordell and Grauch, (1982 & 1985):

$$HG(x, y) = \sqrt{\left(\frac{\partial M}{\partial x}\right)^2 + \left(\frac{\partial M}{\partial y}\right)^2} \quad (1)$$

This function peaks over magnetic contacts under certain assumptions: (1) the magnetic field and source magnetization are vertical, (2) the contact is vertical and (3) the sources are thick (Phillips, 2000). Violation of the first two assumptions leads to shift of the peaks away from the contact location. Violation of the third assumption leads to secondary peaks parallel to that of the contact. When these assumptions are satisfied, the method is effective in detecting lineaments that may correspond to basement faults and contacts. Moreover, the method is less susceptible to noises in the data, because it only requires calculation of the two first-order horizontal derivatives of the magnetic field.

When applied to the reduced-to-pole magnetic data, the horizontal gradient method (Cordell and Grauch, 1985; Blakely and Simpson, 1986; and Roest and Pilkington, 1993) assumes that, the sources are isolated in vertical contacts separating thick geologic units. Peaks in the horizontal gradient magnitude of the reduced-to-pole magnetic field are used to locate the vertical contacts and estimate their strike directions.

The horizontal gradient magnitude (HGM) method is considered as the simplest approach to define the contact locations such as faults, where the maximum horizontal gradient (more properly the maxima of the total horizontal gradient) of the anomaly slope is located near or over the body edge. That is, the horizontal gradient operator in the map form produces maximum ridges over the edges of high dense basement blocks and faults or other dense

bodies. In addition, the horizontal gradient highlights linear features, related to contacts, in the data set.

2-Local Wavenumber Method

The local wavenumber method (also known as source parameter image method SPI) is a technique for calculation of source depths from magnetic data. Local wavenumber is a technique based on the extension of complex analytical signal to estimate magnetic depths. The original SPI method (Thurston and Smith, 1997 and Smith and others, 1998), as implemented by Phillips(2000) assumes that, the sources are isolated and linear, without a presumption of thickness and works for two models: a 2-D sloping contact or a 2-D dipping thin-sheet. For the magnetic field M , the local wavenumber (Thurston and Smith, 1997) is given by:

$$k = \frac{\frac{\partial^2 M}{\partial x \partial z} \frac{\partial M}{\partial x} - \frac{\partial^2 M}{\partial x^2} \frac{\partial M}{\partial z}}{\left(\frac{\partial M}{\partial x}\right)^2 + \left(\frac{\partial M}{\partial z}\right)^2} \quad (2)$$

For the dipping contact, the maxima of k are located directly over the isolated contact edges and are independent of the magnetic inclination, declination, dip, strike and any remnant magnetization. The depth is estimated at the source edge from the reciprocal of the local wavenumber.

$$Depth_{(x=0)} = \frac{1}{k_{\max}} \quad (3)$$

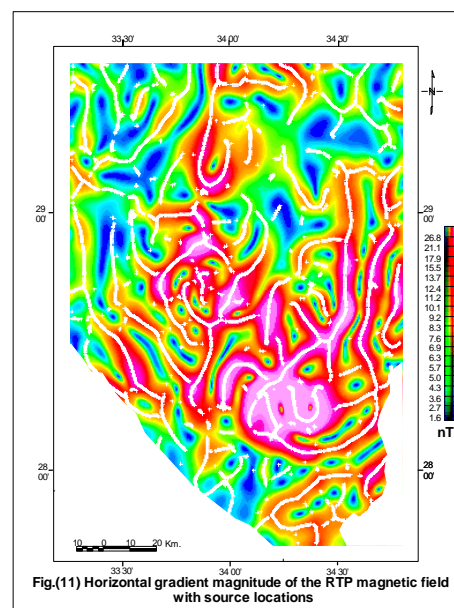
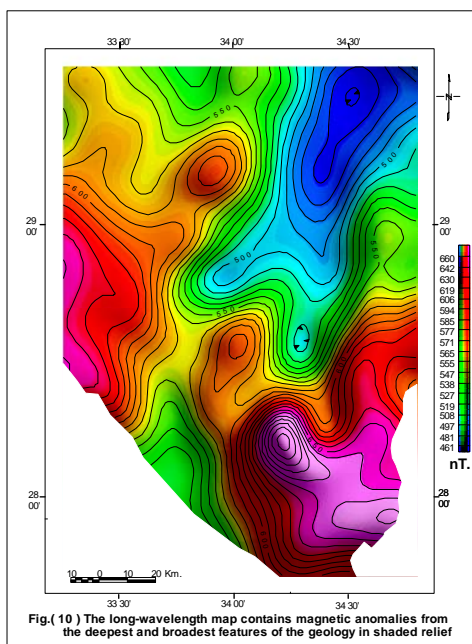
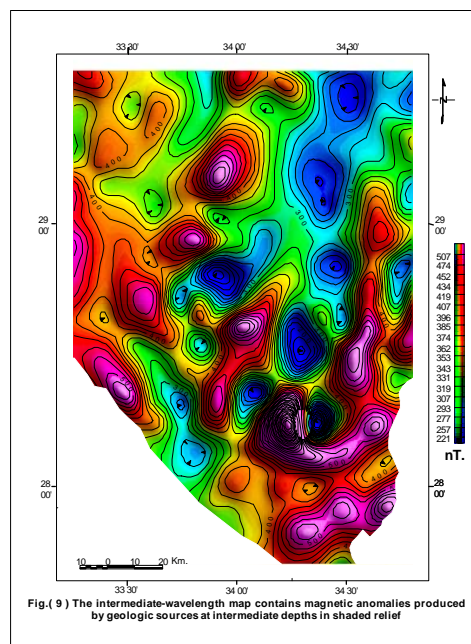
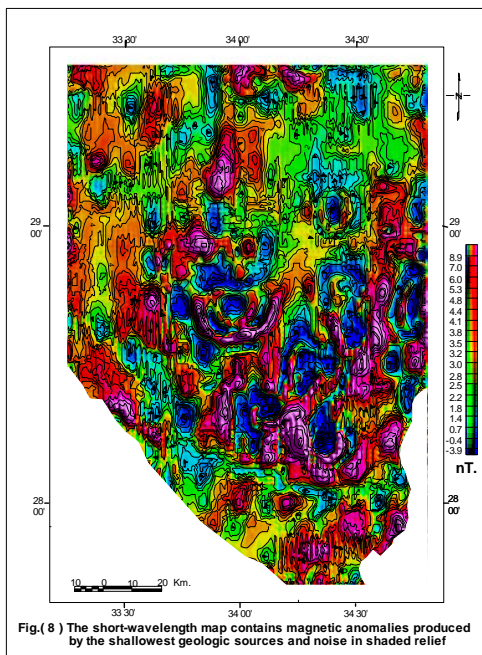
One more advantage of this method is that, the interference of anomaly features is reducible, since the method uses the second-order derivatives. The SPI menu provides options to compute the two horizontal derivative grids in the space-domain, and the first vertical derivative grid in the frequency-domain, using the standard montaj filters and default settings. However, the user may compute these grids separately, if desired.

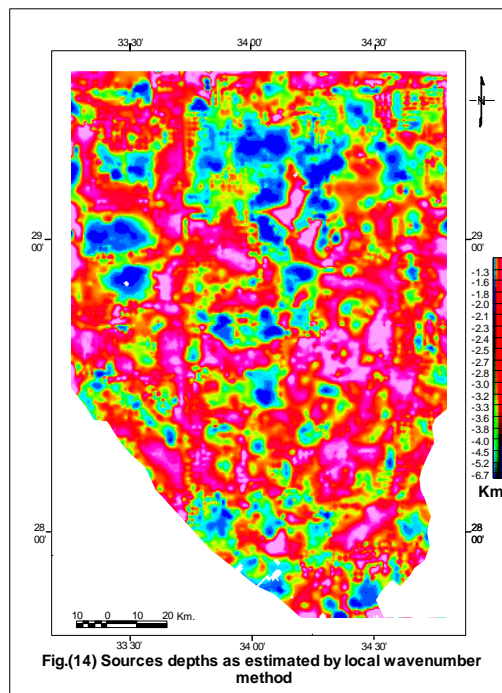
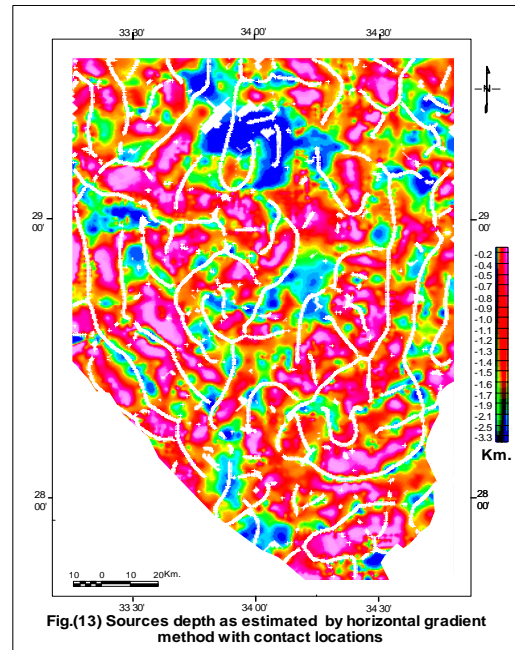
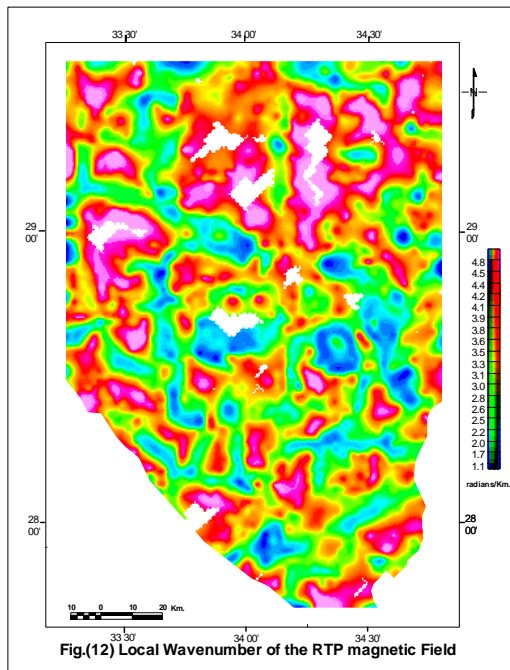
In practice, the method is used on gridded data by first estimating the direction at each grid point. The vertical gradient is computed in the frequency domain, and the horizontal derivatives are computed in the direction perpendicular to the strike using the least-squares method.

The fore-mentioned methods are illustrated for the investigated area. The derivative maps (horizontal gradient and local wavenumber) are shown in the figures (11&12) respectively. Crests of the derivative maps (in white) correspond to the estimated source locations.

On the other hand, the contact locations and depths resulting from the fore mentioned two methods are shown in figures (13&14). The local wavenumber method greatly overestimates the source depths relative to the other one. Otherwise, the two results contain nearly similar features. The inspection of the two maps elucidates the shallow depths at the southeastern and southwestern parts, as well as some separated parts from the central area and another shallow part in the northwestern corner. However, the

deepest depths (from 3.5 to 5.5 km) are located at the central northern part of the area (blue) and at the west central part, as well as other intermediate depths (from 2.5 to 3.5 km) occupied the central and northeastern parts. The shallow depths (ranged from 1.5 to 2.5 km) are illustrated in the other parts of the map area. Generally, the local wavenumber method is quite sensitive to noises in the data to interference effects between nearby sources, which can result in over estimation of the source depths.





Structural evolution

The main target of the magnetic data interpretation of an area is the establishment of the structural features complicating the continuity of the evaluated sedimentary section and the underlying basement complex. Accordingly, the deep-seated structural features and the shallow-seated structural

elements are represented in the study area, belt-wise and zone-wise, as shown as follow:

A-Deep-seated structural features:

The deep-seated structural features of the study area (Fig.15) are integrated as basement swell and trough belts intervened by faults of varying trends. However, the northeastern border of the map

area is concordant with a trough belt of NE-SW trend, which is bifurcated into two splits at its lower end. This trough is formed from two negative features, the first one is trending N-S to the east and the second one trend NNE-SSW at the central part of the map area.

Such a trough belt is followed southeastwardly by, moderate swell through NE-SW and NNW-SSW faults of eastward and westward throws, respectively. Also, that trough belt is followed northwestwardly by a major swell through a NNE-SSW fault of eastward throw.

Added, the fore-mentioned southeastern swell orient mostly NNE-SSW parallel to the Gulf of Aqaba, with mostly NW-SE bifurcation at its southern part, which carved at its northern end. While, the second major northwestern swell is formed from high relief and NE-SW trend with NNW-SSE splitting at its central part toward the northwestern corner. This swell system is bounded by a major NE-SW normal fault to the west and intervened internally by NE-SW and N-S faults throwing inwardly toward the in-between minor trough.

B -Shallow-seated structural elements:

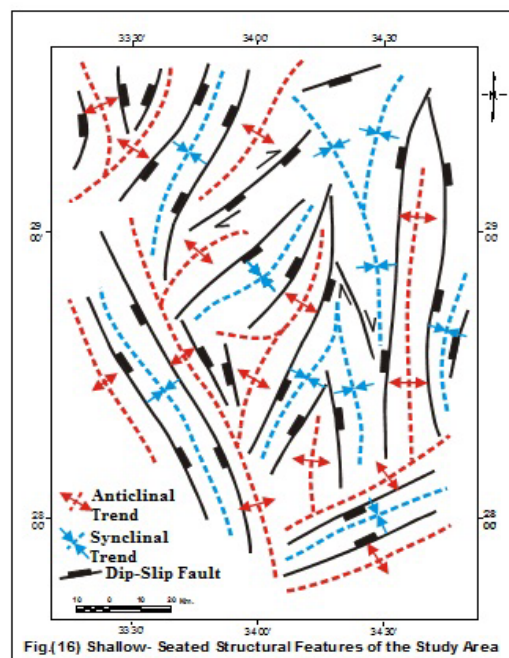
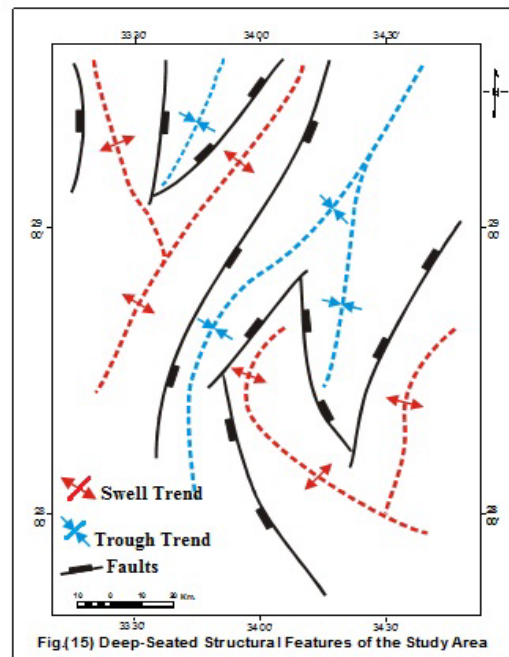
The shallow-seated structural elements of the study area (Fig.16) are cumulated as anticlinal (red colored) and synclinal (blue colored) zones dissected by faults of varying parameters. By this way, the considered area is characterized by the presence of N-S anticlinal zone at the eastern part of the map, followed southwardly by another anticlinal zone orient NE-SW with N-S splitting at the western end.

These anticlinal zones are followed eastwardly by a complex synclinal zone through a N-S fault. This synclinal zone is configured by two segments, northern NNW-SSE one with NNE-SSW split and southern N-S with mostly NE-SW split. The fore-mentioned segments are separated by a NNW-SSE strike-slip fault.

Added, the second NNW-SSE complex anticlinal zone is located to the west of the map area with mostly NE-SW bifurcation at its central part and another NE-SW bifurcation at its northern part. Such a northern split is formed from two segments separated by NE-SW strike-slip fault and followed southwardly and northwardly by two NE-SW low relief synclines through a NE-SW normal fault.

Moreover, other two separate synclinal trends are located at the southwestern corner parallel to the Gulf of Suez and at the southeastern corner parallel to the Gulf of Aqaba. A series of separated NW-SE and NE-SW low extended synclines are observed at the southwestern corner (parallel to the

Gulf of Suez) and southeastern part (Parallel to the Gulf of Aqaba). These synclines are followed outwardly by low relief anticlinal trends in the same directions through normal faults, beside a moderate NE-SW anticlinal zone observed at the northwestern corner, which is formed from two splits (NE-SW and NNW-SSE).



Results and Conclusions

This study was carried out using the available total intensity magnetic data. The data were analyzed using the most advanced and suitable techniques. These techniques include the reduce to the pole filter, low-pass/high-pass filtering, matching band-pass filter, horizontal gradient magnitude and local wave number tool. The phase-shift effects in the total magnetic anomalies resulting from a non-vertical geomagnetic field vector can often be removed using the reduction-to-pole filtering, in which the intended effect is to move the anomaly peaks and gradients directly over their sources to aid in the interpretation.

The magnetic anomalies produced by deep geologic sources can be separated from anomalies produced by shallow geologic effects using power spectrum filtering, and depending on the anomalies wavelength using matched bandpass filtering. Also, the automated interpretation methods can be used to estimate the locations and depths of magnetic sources. Because each automated method makes different assumptions about the sources, the use of several methods is recommended in order to provide a reality check for the results. For that, we used the horizontal gradient and local-wavenumber methods for automatic revealing of the source locations and depths. The application of these tools discriminated the variable sources of specific depth ranges for the residual and regional anomalies. The average depth values to the causative sources are widely ranges between 1 to 5.5 km, as deduced from these derivative methods.

Tectonically, the magnetic methods were critical for detecting the geometry of the basement rocks and the structures related to tectonic forces. The results indicate that the principal tectonic trend is oriented in the NE-SW (N45°-65°E) direction, which connected to Syrian Arc tectonics in this part of the peninsula. The NW-SE (N35°-45° W) tectonic trend is a second order of predominance. This trend originated due to the opening of the Gulf of Suez, and is normal to the NE-SW tension axis (Said,1990). The NNE-SSW (N15°-25°E) tectonic trend, related to Gulf of Aqaba tectonics, can be detected as a third order of predominance. Finally, we can conclude that the area is highly affected by the tectonic related to the Gulf of Suez, Red Sea and Gulf of Aqaba. It is affecting both basement and sedimentary rocks, dividing the study area into several faulted blocks.

Corresponding author

Shadia T. El Khodary
Geology Dept., Faculty of Science, Tanta University,
Tanta, Egypt.
s_elkhodary@hotmail.com

References:

1. Abdelkhalek ML, Abdel Wahed N., and Sehim A.A., 1993: Wrenching deformation and tectonic setting of the northwestern part of the Gulf of Aqaba. Geol. Soc. Egypt Special Pub. 1:409-444.
2. Abu Al-Izz M.S., 1971: Landforms of Egypt. 281p. Dar Al-Maaref, Cairo, Egypt.
3. Agha A., 1981: Structural map and plate reconstruction of the Gulf of Suez-Sinai area. Conoco Oil, Houston.
4. Ahmed FM, Hassaneen AG., 1985: Interpretation of the anomalous geomagnetic field of Egypt with respect to the regional structural of Egypt. NRIAG Bull V(B):101-126.
5. Ben-Menahem A., 1979: Earthquake catalogue for the Middle East (92 B.C.-1980 A.D.). Boll. Geofis. Teor. Appl. 21:245-310.
6. Blakely, R.J., 1995: Potential Theory in Gravity & Magnetic Applications, Cambridge University Press, Cambridge.
7. Blakely, R.J., and Simpson, R.W., 1986: "Approximating edges of source bodies from magnetic or gravity anomalies", Geophysics, v.51, no.7, pp.1494-1498.
8. Cordell, Lindrith, and Grauch, V.J.S., 1982: Mapping basement magnetization zones from aeromagnetic data in the San Juan Basin, New Mexico: Society of Exploration Geophysicists, 52nd Annual Meeting, Abstracts and Bibliographies, p.246-247.
9. Cordell, Lindrith, and Grauch, V.J.S., 1985: Mapping basement magnetization zones from aeromagnetic data in the San Juan basin, New Mexico in Hinze, W.J., ed., The utility of regional gravity and magnetic anomaly maps: Society of Exploration Geophysicists, p.181-197.
10. Freund R., Garfunkel Z., Zak I., and Goldberg M., Weissbrod T., and Darin B., 1970: The shear along the Dead Sea Rift. Philos. Trans. R. Soc. Land A. 267:107-130.
11. Garfunkel Z., 1981: Internal structure of the Dead Sea leaky transform (rift) in relation to plate kinematics- Tectonophysics 80:81-108.
12. Geosoft Program (Oasis Montaj), 2007: Geosoft Mapping and Application System, Inc, Suit 500, Richmond St. West Toronto, ON Canada N5S1V6.
13. Ismail A, Sultan A, Mohamady M., 2001: Bouguer and total magnetic intensity maps of

- Sinai Peninsula. Scale 1:500,000, Proceedings of the 2nd International symposium on Geophysics, Tanta, pp. 111–117.
14. Kora, M., 1995: An introduction to the stratigraphy of Egypt. Lecture notes, Geology Dept. Mansoura Univ., 116pp.
 15. Lyberis N. 1988: Tectonic evolution of the Gulf of Suez and the Gulf of Aqaba. *Tectonophysics* . 153:209-220.
 16. Neev D., 1975: Tectonic evolution of the Middle East and the Levantine basin (eastern most Mediterranean). *Geology* 3:683–686.
 17. Omara, S., 1972: An early Cambrian outcrop in southwestern Sinai, Egypt. *N.J.P. Geol. Palaeontol.* 5, 306-314.
 18. PATTON, T.L., A.R. MOUSTAFA, R.A. NELSON and S.A. ABDINE, 1994: Tectonic evolution and structural setting of the Suez Rift, in *Interior Rift Basins: Tulsa, OK*, edited by S.M. LANDON, *Am. Ass. Pet. Geol. Mem.*, 59, 9-55.
 19. Phillips, J.D., 1997: Potential-field geophysical software for the PC, version 2.2 , U.S. Geological Survey Open-File Report 97-725,
 20. Phillips, J.D., 2000: “Locating magnetic contacts: a comparison of the horizontal gradient, analytic signal, and local wavenumber methods”, *Society of Exploration Geophysicists, Calgary/2000 Technical Program Expanded Abstracts* CD-ROM, (<http://seg.org/meetings/past/seg2000/techprog/pdf/papr0378.pdf>).
 21. Rabeh T., 2003: Structural set-up of Southern Sinai and Gulf of Suez areas indicated by geophysical data. *Annals of Geophysics*, Vol.46, N.6:1325-1337.
 22. Rabeh T., and Miranda M., 2008: A tectonic model of the Sinai Peninsula based on magnetic data. *Journal of Geophysics and Engineering* 5:469-479.
 23. Reilinger R., S. McClusky, A. ArRajehi, S. Mahmoud, A. Rayan, W. Ghebreab, G. Ogubazghi, and A. Al-Aydrus, 2006: Geodetic constraints on rupturing of continental lithosphere along the Red Sea , *Margins Newsletter* 17, 17-21.
 24. Roest, W.R., and Pilkington, Mark, 1993: “Identifying remnant magnetization effects in magnetic data”, *Geophysics*, v.58, no.5, pp.653-659.
 25. Said R., 1990: *The Geology of Egypt*, 2nd edn. Balkema, Rotterdam, pp 439–449.
 26. Smith, R.S., Thurston, J.B., Dai, Ting-Fan, and MacLeod, I.N., 1998: “ISPITM - the improved source parameter imaging method”, *Geophysical Prospecting*, v.46, pp.141-151.
 27. Spector, A., and Grant, F.S., 1970: Statistical models for interpreting aeromagnetic data. *Geophys.*, V. 35, pp. 293-302.
 28. Syberg, F.J.R., 1972: “A Fourier method for the regional-residual problem of potential fields”, *Geophysical Prospecting*, v.20, pp. 47-75.
 29. Thurston, J.B., and Smith, R.S., 1997: “Automatic conversion of magnetic data to depth, dip, and susceptibility contrast using the SPITM method”, *Geophysics*, v.62, no.3, pp.807-813.
 30. U.S. Geological Survey 1998: Open-File Report 99-50-A, U. S. Geological Survey, Denver, Colorado, World Energy Project.

2/9/2011